Inorg. Chem. **2008**, *47*, 5212−5217

Preparation of $Sr_7Mn_4O_{13}F_2$ by the Topotactic Reduction and Subsequent Fluorination of $Sr_7Mn_4O_{15}$

Ian Saratovsky, Michelle A. Lockett, Nicholas H. Rees, and Michael A. Hayward*

Inorganic Chemistry Laboratory, Department of Chemistry, University of Oxford, South Parks Road, Oxford OX1 3QR, United Kingdom

Received January 14, 2008

The topotactic reduction and subsequent fluorination of $Sr_7Mn_4O_{15}$ yields a phase of composition $Sr_7Mn_4O_{13}F_2$. Characterization of this phase utilizing powder neutron diffraction and ^{19}F NMR shows that the fluoride ions are located on a single anion site, the same crystallographic site that is vacant in the reduced intermediate $Sr_7Mn_4O_{13}$.

Introduction

There has been enduring interest in mixed-valent manganese(III/IV) oxides since the observation of large magnetoresistive ratios in these phases. Wide-ranging studies have focused on tuning of the behavior of these phases by cation substitution to optimize the average manganese oxidation state and structural parameters.[1,2] There are, however, relatively few reports of attempts to tune these parameters by substitution on the anion lattice. The few studies that have been reported have focused on the preparation of oxyfluorides via the fluorination of anion-deficient cubic perovskite phases, e.g., the preparation of $Sr_2Mn_2O_5F$ via the fluorination of $Sr_2Mn_2O_5$ or that of Sr_2MnGaO_5F via the fluorination of the brownmillerite Sr_2MnGaO_5.[3,4] The small contrast in the scattering powers of oxide and fluoride ions with respect to X-ray and powder neutron diffraction has made the determination of the anion distribution and/or ordering in oxyfluorides challenging. This problem has been exacerbated by the relatively high symmetry structures adopted by the phases studied, and as a result, the question as to whether the fluorination reactions of reduced oxides are truly topotactic (that is to say, the anion vacancies are simply filled by fluoride ions such that the vacancy ordering patterns the oxide−fluoride distribution) remains open. Understanding this feature of the reactions is critical if we are to utilize anion substitutions effectively to tailor the properties of materials.

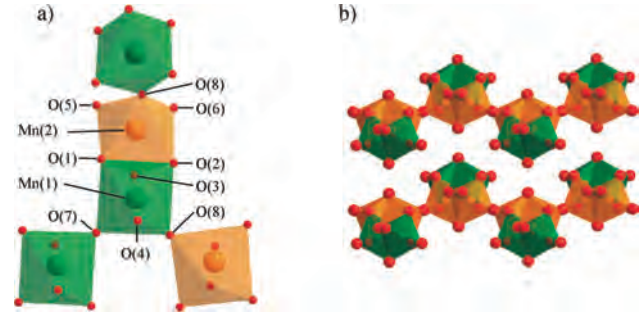

Figure 1. Structure of $Sr_7Mn_4O_{15}$ showing (a) the eight different anion sites in the structure and (b) the layered nature on the Mn−O lattice.

Recently, we have been studying the anion chemistry of a low-symmetry manganese(IV) oxide $Sr_7Mn_4O_{15}$. $Sr_7Mn_4O_{15}$ has a rather complex structure.[5] The manganese oxygen lattice can be thought of as an array of Mn_2O_9 dimers constructed from pairs of MnO_6 octahedra sharing faces (Figure 1a). These Mn_2O_9 units then share corners to form a buckled two-dimensional array (Figure 1b). Low-temperature reduction of this phase with CaH_2 leads to the topotactic deintercalation of oxide ions to form phases of composition $Sr_7Mn_4O_{15-x}$ ($0 < x < 3$).[6,7] The reduced phases retain the topology of the manganese(IV) starting material but have well-defined, highly ordered vacancies in the oxide ion lattice, as shown in Figure 2. The oxide ions are selectively

* To whom correspondence should be addressed. E-mail: michael.hayward@chem.ox.ac.uk.

(1) Rao, C. N. R.; Cheetham, A. K.; Mahesh, R. *Chem. Mater.* **1996**, *8*, 2421.
(2) Raveau, B.; Maignan, A.; Martin, C.; Hervieu, M. *Chem. Mater.* **1998**, *10*, 2641.
(3) Lobanov, M. V.; Abakumov, A. M.; Sidorova, A. V.; Rozova, M. G.; D'yachenko, O. G.; Antipov, E. V.; Hadermann, J.; Van Tendeloo, G. *Solid State Sci.* **2002**, *4*, 19–22.
(4) Alekseeva, A. M.; Abakumov, A. M.; Rozova, M. G.; Antipov, E. V.; Hadermann, J. *J. Solid State Chem.* **2004**, *177*, 731–738.
(5) Vente, J. F.; Kamenev, K. V.; Sokolov, D. A. *Phys. Rev. B* **2001**, *64*, 214403.
(6) Hayward, M. A. *Chem. Commun.* **2004**, 170.
(7) O'Malley, M.; Lockett, M. A.; Hayward, M. A. *J. Solid State Chem.* **2007**, *180*, 2851–2858.

10.1021/ic800066g CCC: $40.75
Published on Web 05/10/2008

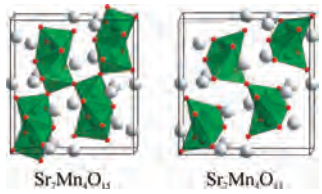

Figure 2. Structural relationship between $Sr_7Mn_4O_{15}$ and $Sr_7Mn_4O_{13}$.

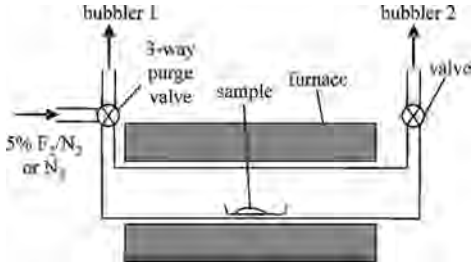

Figure 3. Apparatus used from the fluorination of $Sr_7Mn_4O_{15-x}$ samples.

removed from the apex-shared anion sites, initially from site O(8) to form $Sr_7Mn_4O_{13}$ and then from site O(7) to form $Sr_7Mn_4O_{12}$. The topotactic fluorination of these phases should, therefore, result in a mixed-valent manganese(III/IV) oxyfluoride with sufficiently low crystal symmetry to allow for the determination of the anion distribution on the basis of differing Mn−F and Mn−O bond lengths.

Experimental Section

Five gram samples of $Sr_7Mn_4O_{15}$ were prepared via a citrate precursor method. Suitable quantities of $SrCO_3$ (99.994%) and MnO_2 (99.999%) were dissolved in 100 mL of a 1:1 mixture of 6 M nitric acid and distilled water. A total of 10 mol equiv of citric acid and 5 mL of analar ethylene glycol were added, and the solution was heated with constant stirring. The gel thus formed was subsequently ground into a fine powder, placed in an alumina crucible, and heated at 1 °C min^{-1} to 1000 °C in air. The resulting black powder was then pressed into 13 mm pellets at 5 tonnes pressure and heated in air at 1350 °C for 2 × 2 days with regrinding between heating periods. Powder X-ray diffraction data collected from samples could be indexed on the basis of a monoclinic cell (space group $P2_1/c$) and gave lattice parameters [$a = 6.8124(2)$ Å, $b = 9.6152(4)$ Å, $c = 10.3744(4)$ Å, $\beta = 91.865(3)°$] in good agreement with previously reported values for $Sr_7Mn_4O_{15}$.[5] Samples of composition $Sr_7Mn_4O_{15-x}$ ($2 < x < 3$) were prepared by the reduction of $Sr_7Mn_4O_{15}$ with CaH_2 in the temperature range 300 °C $< T <$ 370 °C as described previously.[7]

Fluorination of $Sr_7Mn_4O_{15-x}$. Samples of $Sr_7Mn_4O_{15-x}$, prepared as described above, were fluorinated using a 5% F_2/N_2 gas mixture (BOC gases). Samples of $Sr_7Mn_4O_{15-x}$ contained in alumina boats were loaded, in an argon-filled glovebox, into a silica tube with valves at each end. The tube was then removed from the glovebox and connected, as shown in Figure 3. Initially, the tubing prior to the reaction volume was purged with dry nitrogen through bubbler 1 via a three-way purge valve to remove all oxygen from the system. Subsequently, the sample volume, sealed from the atmosphere by bubbler 2, was also purged. The gas flow was then changed to a 5% F_2 in N_2 mixture and the system purged for a further 5 min. Either the sample was then heated under flowing F_2/N_2 or through closure of the three-way purge valve the sample was heated under the static atmosphere trapped in the reaction tube by bubbler 2. It should be noted that the downstream valve between the sample and bubbler 2 was left open to allow the reaction gas to expand upon heating. A large sample of $Sr_7Mn_4O_{13}$ (~2.5 g) was fluorinated by multiple exposures to a static 5% F_2/N_2 atmosphere such that the total quantity of F_2 exposed to the sample conformed to the desired 1:1 molar ratio.

Characterization. Powder X-ray diffraction data were collected from samples contained within homemade air-sensitive sample holders utilizing a PANalytical X'Pert diffractometer incorporating an X'celerator position-sensitive detector (monochromatic Cu $K\alpha_1$ radiation). Powder neutron diffraction data were collected at room temperature from samples contained within vanadium cans that had been sealed under nitrogen with an indium washer. Data were collected using the D2B diffractometer ($\lambda = 1.59$ Å) at the ILL facility, Grenoble, France. Structural refinements were preformed by utilizing the GSAS suite of programs.[8] Average manganese oxidation states in all samples were determined by dissolution in HCl containing an excess of KI and titration of the liberated I_2 with $Na_2S_2O_3$.

^{19}F NMR magic angle spinning (MAS) spectra were acquired at 376.2 MHz on a Varian/Chemagnetics Infinity spectrometer equipped with a 4 mm double-resonance probe. Samples were packed in 4 mm o.d. rotors and spun at a MAS rate between 14 and 17 kHz using dry nitrogen for all gas requirements. Typically, 2000 transients were acquired with an acquisition time of 0.512 ms (512 data points zero filled to 32 768), a sweep width of 1000 kHz, and a recycle delay of 5 s. The ^{19}F NMR background signal from the probe was suppressed using the DEPTH[9] pulse sequence. All spectra were externally referenced to Teflon (where the Teflon resonance is taken to be at $\delta = -123.2$ ppm) on a scale where $\delta(CFCl_3) = 0$ ppm.

Results

Powder X-ray diffraction data collected from $Sr_7Mn_4O_{15-x}$ samples were readily indexed with cells consistent with previous reports.[7] The lattice parameters thus obtained are shown in Table 1 with the chemical composition of the phases, determined by iodometric titration. No evidence for impurity phases was observable in these data sets.

Reactivity of $Sr_7Mn_4O_{15-x}$ ($x = 2, 3$) with Fluorine. Heating samples of composition $Sr_7Mn_4O_{15-x}$ ($2 < x < 3$) under a flow of 5% F_2/N_2 below 200 °C resulted in no reaction. Above this temperature, a yellow solid was formed, whose powder X-ray diffraction revealed a mixture of SrF_2 and a rhombohedral phase [$a = 7.092(3)$ Å, $c = 6.791(3)$ Å, and $\gamma = 120°$]. This phase was identified as $SrMnF_6$, by analogy to $SrNiF_6$ and $SrCrF_6$.[10,11] Full structural details of this new phase will be reported elsewhere. This suggests that the reaction described in eq 1 is occurring.

$$Sr_7Mn_4O_{13} + 15F_2 \rightarrow 3SrF_2 + 4SrMnF_6 + 6.5O_2 \quad (1)$$

In order to avoid overfluorination to a fluoride rather than formation of an oxyfluoride, samples of $Sr_7Mn_4O_{15-x}$ were heated under a static F_2/N_2 atmosphere as described above. This allowed the stoichiometric ratio of $Sr_7Mn_4O_{15-x}/F_2$ to be fixed at the value required for simple topotactic

(8) Larson, A. C.; Von Dreele, R. B. General Structure Analysis System. Los Alamos National Laboratory Report LAUR 86-748, **2000**.
(9) Cory, D. G.; Ritchey, W. M. *J. Magn. Reson.* **1088**, *80*, 128–132.
(10) Hoppe, R.; Fleisher, T. *J. Fluorine Chem.* **1978**, *11*, 251–264.
(11) Siebert, G.; Hoppe, R. *Z. Anorg. Allg. Chem.* **1972**, *391*, 126–136.

Table 1. Lattice Parameters and Chemical Compositions of $Sr_7Mn_4O_{15-x}$ Phases

sample no.	a (Å)	b (Å)	c (Å)	β (deg)	volume (Å^3)	average Mn oxidation state	implied composition
1	6.8669(6)	9.8017(9)	10.0957(9)	94.138(1)	677.7(1)	+3.00(1)	$Sr_7Mn_4O_{13(2)}$
2	6.9252(2)	9.7222(3)	10.0527(3)	93.695(2)	675.44(6)	+2.63(1)	$Sr_7Mn_4O_{12.27(2)}$
3	6.954(1)	9.674(2)	10.041(2)	93.31(1)	674.3(4)	+2.51(1)	$Sr_7Mn_4O_{12.02(2)}$

Table 2. Lattice Parameters and Chemical Compositions of Fluorinated $Sr_7Mn_4O_{15-x}$

sample no.	a (Å)	b (Å)	c (Å)	β (deg)	volume (Å^3)	average Mn oxidation state	implied composition
1	6.8348(6)	9.6330(8)	10.433(1)	91.933(6)	686.7(1)	+3.52(1)	$Sr_7Mn_4O_{13}F_{2.00(4)}$
2	6.851(1)	9.621(2)	10.563(2)	91.766(9)	696.0(4)	+3.31(1)	$Sr_7Mn_4O_{12.25(4)}F_{2.75(4)}$
3	6.814(1)	9.578(1)	10.402(1)	91.76(1)	678.5(2)	+3.25(1)	$Sr_7Mn_4O_{12.00(4)}F_{3.00(4)}$

fluorination (1:1 for $Sr_7Mn_4O_{13}$ and 1.5:1 for $Sr_7Mn_4O_{12}$). Heating samples under a static 5% F_2/N_2 atmosphere at 300 °C resulted in the formation of mixtures containing large quantities of poorly crystalline SrF_2 and binary manganese oxides. Raising the reaction temperature to 350 °C, however, resulted in much cleaner reactions with no SrF_2 observable by powder X-ray diffraction for the reaction with $Sr_7Mn_4O_{13}$ and only a small amount (~6 mol %) for the reaction with more reduced $Sr_7Mn_4O_{13-x}$ samples. Powder X-ray diffraction data collected from these fluorinated phases could be indexed on the basis of monoclinic unit cells listed in Table 2. These values are consistent with the simple topotactic fluorination of the substrate phases.

High-temperature annealing (1000 °C) of the fluorinated samples under vacuum leads to decomposition of all phases and the formation of SrF_2 and Sr_2MnO_{4-x} among other products, confirming the presence of fluorine in all samples. Iodometric titration measurements indicate average manganese oxidation states for the fluorinated samples shown in Table 2. These are consistent with complete fluorination from $Sr_7Mn_4O_{15-x}$ to $Sr_7Mn_4O_{15-x}F_x$.

Structural Characterization of Fluorinated $Sr_7Mn_4O_{13}$. Powder neutron diffraction data collected from a sample of $Sr_7Mn_4O_{13}$, fluorinated as described above, could be readily indexed using a monoclinic unit cell consistent with $P2_1/c$ symmetry, suggesting that a topotactic oxidation with fluorine has been achieved. A structural model based on that of $Sr_7Mn_4O_{15}$ (anion labels shown in Figure 1) but with a fluoride ion located in the O(8) position (a choice that will be discussed in detail later) was refined against the powder neutron diffraction data. Initial refinement cycles resulted in a reasonably good fit to the data. Close inspection, however, revealed a number of diffraction reflections that were not accounted for by the model but that were consistent with small quantities of SrF_2 in the sample. SrF_2 was, therefore, added to the model as a second phase, leading to significant improvement in the agreement between observed and calculated data sets. Initially, the Sr(3) site was located on the high-symmetry 2d ($^1/_2$, 0, $^1/_2$) position within the model; however, a large displacement parameter refined for this atom suggested that it was disordered over the lower-symmetry 4e site observed in the structure of $Sr_7Mn_4O_{15}$.[5] Adding this change to the model led to a small but statistically significant improvement in the fit to the data, and so it was retained. The analogous disordering of the O(7) site also observed in the $Sr_7Mn_4O_{15}$ structure led to a worsening of goodness of fit parameters so the high-symmetry description was retained.

Table 3. Refined Structure of $Sr_7Mn_4O_{13}F_2$[a]

	x	y	z	fraction	U_{iso}
Sr(1)	0.990(1)	0.189(1)	0.4625(9)	1	0.013(1)
Sr(2)	0.343(2)	0.1523(1)	0.199(1)	1	0.013(1)
Sr(3)	0.511(4)	0.007(3)	0.538(2)	0.5	0.013(1)
Sr(4)	0.176(2)	0.003(1)	0.835(1)	1	0.013(1)
Mn(1)	0.585(3)	0.167(2)	0.925(1)	1	0.011(3)
Mn(2)	0.767(3)	0.174(2)	0.731(1)	1	0.011(3)
O(1)	0.518(2)	0.100(1)	0.760(1)	1	0.009(1)
O(2)	0.677(2)	0.175(1)	0.338(1)	1	0.009(1)
O(3)	0.834(2)	0.093(1)	0.890(1)	1	0.009(1)
O(4)	0.336(3)	0.242(1)	0.937(1)	1	0.017(2)
O(5)	0.856(2)	0.024(1)	0.623(1)	1	0.017(2)
O(6)	0.018(3)	0.248(1)	0.698(1)	1	0.017(2)
O(7)	0.5	0	0	1	0.033(7)
F	0.669(1)	0.228(1)	0.074(1)	1	0.005(1)

[a] Space group $P2_1/c$, $a = 6.8355(6)$ Å, $b = 9.6335(8)$ Å, $c = 10.435(1)$ Å, $\beta = 91.941(7)°$, volume = 686.5(1) Å^3, mole fraction = 96.2(3)%. SrF_2: $Fm\bar{3}m$, $a = 5.808(1)$ Å, mole fraction = 3.8(2)%. $\chi^2 = 2.05$, $wR_p = 5.303\%$, $R_p = 4.17\%$.

In the final refinement cycles, atomic positions and isotropic displacement parameters were refined for all atoms. The displacement parameters of the cations were constrained by element, and those of the anions were constrained by bonding configuration (face-sharing, nonbridging; the two corner-sharing sites were allowed to refine independently) to assist in refinement stability. Refinement of the anion fractional occupancies resulted in values consistent with full occupancy of all sites within error. Full details of the refined structure and selected bond lengths are detailed in Tables 3 and 4 with a comparison of the observed data and calculated fit shown in Figure 4.

Solid-State NMR Characterization of $Sr_7Mn_4O_{13-x}F_{2+x}$ Phases. The solid-state ^{19}F MAS NMR data collected from a sample of $Sr_7Mn_4O_{13}F_2$ contains a single very broad spinning side-band manifold (Figure 5a) with a central isotropic peak [$\delta^{19}(F) = -87.6$ ppm, marked with an asterisk]. Such a broad signal is expected from a fluorine center in close proximity to a paramagnetic manganese ion. The extreme broadness of the spectrum, however, raised some doubts as to whether the signal was due to the paramagnetic broadening of the resonance from a single fluorine environment or whether it was made up from a number of different resonances from fluoride ions in subtly different environments, as would be expected if the fluoride ions were distributed over a number of different anion sites.

In order to break this ambiguity, data were also collected from samples of composition $Sr_7Mn_4O_{12.27}F_{2.73}$ and

Table 4. Selected Bond Lengths Calculated from the Structure of $Sr_7Mn_4O_{13}F_2$

	$Sr_7Mn_4O_{13}F_2$		
cation	anion	bond length (Å)	BVS
Mn(1)	O(1)	1.88(1)	+4.40
	O(2)	1.89(2)	
	O(3)	1.89(2)	
	O(4)	1.85(2)	
	O(7)	1.88(1)	
	F	1.74(1)	
Mn(2)	O(1)	1.87(2)	+3.80
	O(2)	1.94(2)	
	O(3)	1.87(1)	
	O(5)	1.94(2)	
	O(6)	1.90(2)	
	F	1.98(1)	
Sr(1)	O(2)	2.46(1)	+2.23
	O(3)	2.46(1)	
	O(4)	2.48(2)	
	O(5)	2.48(1)	
	O(5)	2.50(1)	
	O(6)	2.83(1)	
	O(6)	2.52(1)	
	F	2.64(1)	
Sr(2)	O(1)	2.63(1)	+2.11
	O(1)	2.73(1)	
	O(2)	2.67(2)	
	O(3)	2.79(1)	
	O(4)	2.86(1)	
	O(4)	2.68(1)	
	O(5)	2.88(1)	
	O(6)	2.42(2)	
	O(7)	2.78(1)	
	F	2.72(1)	
Sr(3)	O(1)	2.48(2)	+1.83
	O(1)	3.27(2)	
	O(2)	2.91(2)	
	O(2)	2.53(2)	
	O(4)	2.86(3)	
	O(4)	2.78(3)	
	O(5)	2.95(3)	
	O(5)	2.52(3)	
	F	2.80(3)	
	F	3.15(2)	
Sr(4)	O(1)	2.66(1)	+1.79
	O(2)	2.70(1)	
	O(3)	3.01(1)	
	O(3)	2.57(1)	
	O(4)	2.74(1)	
	O(5)	3.06(2)	
	O(6)	2.80(1)	
	O(6)	2.94(1)	
	O(7)	2.75(1)	
	F	2.62(1)	

$Sr_7Mn_4O_{12}F_3$. These more extensively fluorinated samples must have fluoride ions on more than one crystallographic site because of the low multiplicity of the anion sites in the structure. Thus, if the single broad resonance observed for $Sr_7Mn_4O_{13}F_2$ is from a single fluorine environment, we would expect to see one, or more, additional fluorine signals for the $Sr_7Mn_4O_{13-x}F_{2+x}$ samples as additional anion sites are substituted.

Parts b and c of Figure 5 show the ^{19}F NMR data collected from $Sr_7Mn_4O_{12.27}F_{2.73}$ and $Sr_7Mn_4O_{12}F_3$, respectively. It can clearly be seen that both data sets contain an additional resolved broad spinning side-band manifold, with an isotropic chemical shift of $\delta^{19}(F) = -108.7$ ppm (as indicated by red markers), with respect to the $Sr_7Mn_4O_{13}F_2$ data. This is consistent with the presence of two fluorine environments

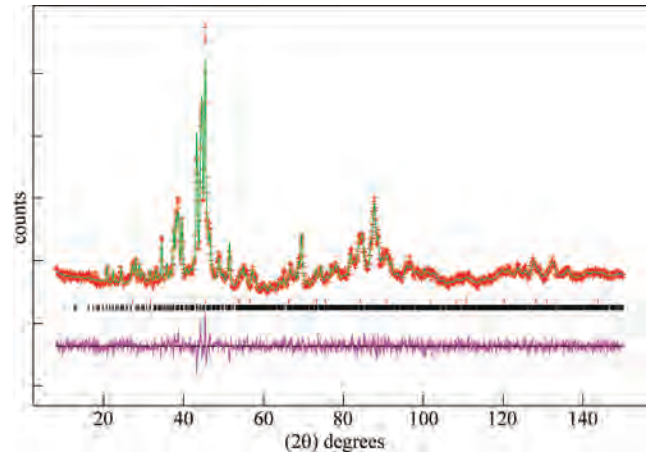

Figure 4. Observed calculated and difference plots from the structural refinement of $Sr_7Mn_4O_{13}F_2$ against powder neutron diffraction data.

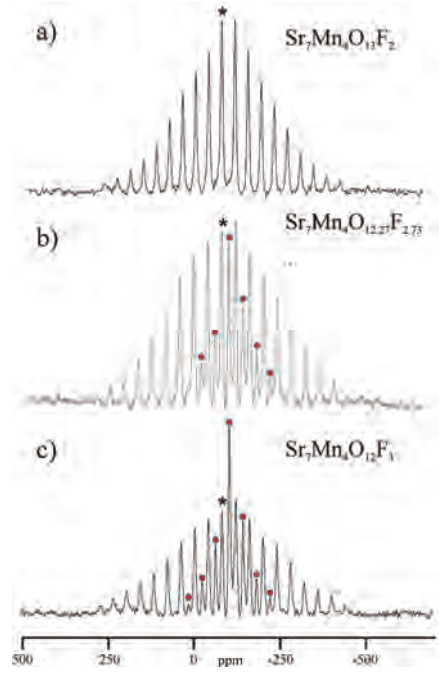

Figure 5. ^{19}F NMR data collected from $Sr_7Mn_4O_{13-x}F_{2+x}$ samples. The asterisk marks the central isotropic peak. The red markers in parts b and c indicate peaks from the second resonance not present in part a.

in these phases: that already observed for $Sr_7Mn_4O_{13}F_2$ and a second, new environment. The size of this new signal can be seen to scale with the amount of additional fluorine added to the samples as expected. These observations unambiguously show that fluoride ions are present on a single crystallographic site within the structure of $Sr_7Mn_4O_{13}F_2$ and two distinct sites in the $Sr_7Mn_4O_{13-x}F_{2+x}$ phases.

Discussion

Reactivity of $Sr_7Mn_4O_{13-x}$ Phases with F_2. The reaction of $Sr_7Mn_4O_{13-x}$ phases with a stoichiometric excess of fluoride to form $SrMnF_6$ and SrF_2 can be seen as a demonstration of the high relative stability of manganese(IV) centers in polar solids. There are, however, relatively few manganese(IV) fluorides known, so similar anion displacement reactions of ternary oxides with excess fluoride could provide a useful route to phases of this kind.

The reactivity of the $Sr_7Mn_4O_{13-x}$ phases with a stoichiometric quantity of fluorine is also slightly unusual. At low temperature ($T \leq 300$ °C), only SrF_2 and MnO_x phases are produced, consistent with a surface-only reaction between F_2 and the substrate oxide. A temperature of 350 °C is required for the insertion of fluoride ions into the structure reminiscent of the staging observed in more conventional intercalation reactions and suggesting that there is a significant kinetic barrier to the reaction, presumably arising from the required lattice expansion.

Structure of $Sr_7Mn_4O_{15-x}F_x$ Phases. The inability to produce large samples (>2 g) of $Sr_7Mn_4O_{15-x}F_x$ ($x > 2$) prevented the collection of powder neutron diffraction data from these phases. Given the relative X-ray scattering powers of strontium, manganese, oxygen, and fluorine, it is impossible to gain a meaningful description of the structure of these phases from X-ray diffraction data alone, so we will limit our discussion to $Sr_7Mn_4O_{13}F_2$.

Inspection of the crystal structure refined against powder neutron diffraction data for $Sr_7Mn_4O_{13}F_2$ reveals that it has the same topology as $Sr_7Mn_4O_{15}$; however, as noted above, the contrast in scattering power between oxide and fluoride ions with either X-ray or neutron diffraction is very small. It is, therefore, not possible to determine the anion distribution in a mixed oxide−fluoride phase with any confidence based on the scattering powers of crystallographic sites alone. We have, therefore, employed a range of different characterization techniques to gain additional information about the anion distribution in this phase.

Fluorination of $Sr_7Mn_4O_{13}$ yields a phase that has full anion site occupancy, as determined by neutron diffraction. High-temperature annealing (1000 °C) under vacuum leads to decomposition of the phase and the formation of SrF_2 and Sr_2MnO_{4-x} among other products. Thus, we are confident that the material contains both oxygen and fluorine; that is to say, it has a composition $Sr_7Mn_4X_{15}$ (X = O, F). Iodometric titration indicates that the sample has an average manganese oxidation state of +3.52. This is consistent with a stoichiometry of $Sr_7Mn_4O_{13}F_2$, which would be the expected product of the simple topotactic oxidation of $Sr_7Mn_4O_{13}$ with fluorine. Solid-state ^{19}F NMR data collected from the material show a single resonance, indicating that all of the fluoride ions are in the same environment; that is to say, they are ordered on the same crystallographic site rather than distributed over a number of anion sites. This information immediately rules out anion site O(7) as the location of the fluoride ions because it has a site multiplicity of 2 per cell, or 1 per formula unit. Complete filling of this site with fluoride ions would only achieve a stoichiometry of $Sr_7Mn_4O_{14}F$, inconsistent with the titration data. We can, therefore, deduce that the fluoride ions are located on one of the remaining 4e anion sites.

The complex low-symmetry structure of $Sr_7Mn_4X_{15}$ phases makes the analysis of factors that affect the bonding and packing in these materials very complex. A great deal of information can, however, be gleaned by the analysis of the small structural differences between phases. Such

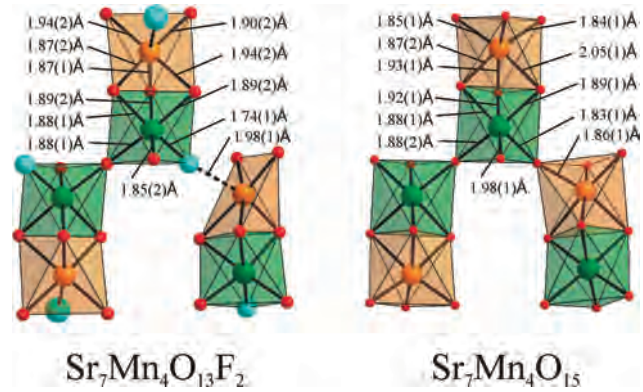

Figure 6. Comparison of the Mn−X lattices of $Sr_7Mn_4O_{13}F_2$ and $Sr_7Mn_4O_{15}$.[5]

a comparison of the structures of $Sr_7Mn_4O_{15}$ and $Sr_7Mn_4O_{13}F_2$ reveals a number of striking differences, as shown in Figure 6.

The most obvious difference is the displacement of the O(8) anion site from a position that is essentially equally disposed between the Mn(1) and Mn(2) sites in the structure of $Sr_7Mn_4O_{15}$ to one that is much closer to the Mn(1) position in $Sr_7Mn_4O_{13}F_2$ [O(8)−Mn(1)/O(8)−Mn(2) = 1.83(1) Å/1.86(1) Å as opposed to 1.74(1) Å/1.98(1) Å for $Sr_7Mn_4O_{15}$ and $Sr_7Mn_4O_{13}F_2$, respectively], as shown in Figure 6. The validity of this anion displacement was confirmed by insertion of an additional anion site at the equal and opposite displacement from the "equal bond" position. Upon combined refinement of the fractional occupancy and positional parameters of this new site and the existing O(8) position, either the fractional occupancy of the new site declined to zero or the new site migrated to the existing O(8) position, demonstrating that the displacement from the "equal bond" position is ordered rather than disordered. The particularly short contact between Mn(1) and O(8) sites [1.76(1) Å] is consistent with a Mn^{IV}−F bond rather than a Mn^{IV}−O contact (Mn^{IV}−F = 1.73−1.78 Å for $A^I_2Mn^{IV}F_6$; Mn^{IV}−O = 1.87−1.90 Å for $A^{II}MnO_3$[12,15]), indicating that the fluoride ions in the structure are located on this site.

The large difference between the Mn(1)−F(8) and Mn(2)−F(8) bond lengths is suggestive of a degree of charge ordering, with Mn^{IV} ions located on the Mn(1) site and Mn^{III} ions located on the Mn(2) site. This assertion is reinforced by the differing bond valence sums (BVSs)[16] calculated for the two sites [Mn(1) = +4.40 and Mn(2) = +3.80 calculated using the parameters for Mn^{IV} and all anions being oxide). It would, however, be expected that localized six-coordinate manganese(III) centers would exhibit a Jahn−Teller distortion, which is not observed. This distortion could be suppressed by the face-sharing connectivity of the $Mn(O/F)_6$ polyhedra, or its absence could be seen as an indication that any charge localization in the structure is incomplete. It

(12) Hoppe, R.; Hofmann, B. *Z. Anorg. Allg. Chem.* **1977**, *436*, 65–74.
(13) Battle, P. D.; Gibb, T. C.; Jones, C. W. *J. Solid State Chem.* **1988**, *74*, 60–66.
(14) Cussen, E. J.; Battle, P. D. *Chem. Mater.* **2000**, *12*, 831–838.
(15) Poeppelmeier, K. R.; Leonowicz, M. E.; Scanlon, J. C.; Longo, J. M.; Yelon, W. B. *J. Solid State Chem.* **1982**, *45*, 71.
(16) Brese, N. E.; O'Keefe, M. *Acta Crystallogr., Sect. B: Struct. Sci.* **1991**, *B47*, 192–197.

is not surprising that the absolute value of the BVS calculated for the two manganese sites is unrealistically large. Phases prepared by the topotactic manipulation of the anion lattice often have unrealistic values. This is because in this instance one could consider the $Sr_7Mn_4O_{15}$ structure optimized for Sr^{2+}, Mn^{4+}, and O^{2-} ions rather than Sr^{2+}, $Mn^{3+/4+}$, O^{2-}, and F^- ions and so, within the restriction preventing long-range cation diffusion, the structure will distort to adopt the lowest-energy configuration. The resulting cation coordination polyhedra are, therefore, likely to differ significantly from those in phases prepared at high temperature under equilibrium conditions, which are free to change the large-scale structure of the phase to adopt idealized coordination geometries. Although it is, therefore, not possible to use the absolute value of BVSs to indicate likely cation oxidation states, comparison of BVS values calculated for different cation sites resident in the same structure is instructive. In this instance the large difference in BVS values calculated for the Mn(1) and Mn(2) sites is significant and requires some explanation, the most plausible explanation being a degree of charge ordering.

The above observations suggest a chemical model in which the fluorination of the manganese(III) phase $Sr_7Mn_4O_{13}$ leads to the formation of the manganese(III/IV) phase $Sr_7Mn_4O_{13}F_2$. The fluoride ions are inserted topotactically into the structure and reside on the anion site from which oxide ions were originally removed on the reduction of $Sr_7Mn_4O_{15}$ to $Sr_7Mn_4O_{13}$. The fluoride ions bond to the two manganese cation sites unevenly, suggesting a degree of charge ordering. Manganese(III/IV) charge ordering is relatively common in cubic perovskites[17] but is largely unknown in materials based on the hexagonal perovskite structure, the exception being phases with manganese coordination sites that have different coordination numbers.

The driving force for locating the fluoride ions on the vacant O(8) site is unclear. Although a kinetic explanation is attractive, it is far from water tight because the fluorination reaction occurs at 350 °C, which is higher than the reduction temperature at which $Sr_7Mn_4O_{13}$ is reduced to $Sr_7Mn_4O_{12}$,[6,7] indicating that the oxide ion lattice is potentially highly mobile. Thus, rather than filling up the vacant sites in a rigid, static anion lattice, the whole anion lattice could, in principle, be free to rearrange itself, as has been seen recently during the reduction of $SrFeO_{2.85}$ to $SrFeO_2$ at 280 °C.[18] An alternative explanation for the selectivity in the oxygen/fluorine distribution is that the same forces that lead to the selectivity in the distribution of anion vacancies upon reduction of $Sr_7Mn_4O_{15}$, namely, the opposing coordination requirements of the strontium and manganese cations,[7] also direct the distribution of the fluoride ions in the structure. It is beyond the scope of this study to differentiate between these two models, but it is clearly striking that the fluoride ions adopt such an ordered distribution.

In conclusion, the sequential topotactic reduction and fluorination of $Sr_7Mn_4O_{15}$ allows the preparation of a mixed-valent manganese(III/IV) phase with an ordered oxygen−fluorine lattice. This "reduce then oxidize" approach is expected to allow the preparation of a large number of oxyfluorides and offers the prospect of patterning the oxygen−fluorine ordering in such phases via control of the anion vacancy ordering in the reduced intermediates.

Acknowledgment. We thank E. Suard for assistance in collecting the neutron power diffraction data and the EPSRC for funding.

IC800066G

(17) Rao, C. N. R.; Raveau, B. *Colossal Magnetoresistance, Charge Ordering and Related Properties of Manganese Oxides*; World Scientific: Singapore, 1998.

(18) Tsujimoto, Y.; Tassel, C.; Hayashi, N.; Watanabe, T.; Kageyama, H.; Yoshimura, K.; Takano, M.; Ceretti, M.; Ritter, C.; Paulus, W. *Nature* **2007**, *450*, 1062–1065.